Solid State Phenomena
ISSN: 1662-9779, Vol. 362, pp 7-12
doi:10.4028/p-dInd9N

Submitted: 2023-09-05
Revised: 2024-04-08
Accepted: 2024-04-08
Online: 2024-08-27

Vertical Current Transport in Monolayer MoS_2 Heterojunctions with 4H-SiC Fabricated by Sulfurization of Ultra-Thin MoO_x Films

Salvatore Ethan Panasci[1,a], Emanuela Schilirò[1,b], Marco Cannas[2,c], Simonpietro Agnello[2,d], Antal Koos[3,e], Miklos Nemeth[3,f], Béla Pécz[3,g], Fabrizio Roccaforte[1,h], Filippo Giannazzo[1,i*]

[1]CNR-IMM, Strada VIII 5 95121, Catania, Italy

[2]Department of Physics and Chemistry Emilio Segré, University of Palermo, Via Archirafi 36, Palermo 90143, Italy

[3]Centre for Energy Research, Institute of Technical Physics and Materials Science, Konkoly-Thege ut 29–33, Budapest 1121, Hungary

[a]SalvatoreEthan.Panasci@imm.cnr.it, [b]Emanuela.Schiliro@imm.cnr.it, [c]marco.cannas@unipa.it, [d]simonpietro.agnello@unipa.it, [e]koos.antal@energia.mta.hu, [f]nemeth.miklos@energia.mta.hu, [g]pecz.bela@energia.mta.hu, [h]fabrizio.roccaforte@imm.cnr.it, [i*]Filippo.Giannazzo@imm.cnr.it

*corresponding author

Keywords: MoS_2, 4H-SiC, heterojunctions, Raman, conductive AFM, diodes

Abstract. In this paper, we report on the growth of highly uniform MoS_2 films, mostly consisting of monolayers, on SiC surfaces with different doping levels (n- SiC epitaxy, ~10^{16} cm^{-3}, and n^+ SiC substrate, ~10^{19} cm^{-3}) by sulfurization of a pre-deposited ultra-thin MoO_x films. MoS_2 layers are lowly strained (~0.12% tensile strain) and highly p-type doped ($<N_h>\approx 4\times10^{19}$ cm^{-3}), due to MoO_3 residues still present after the sulfurization process. Nanoscale resolution I-V analyses by conductive atomic force microscopy (C-AFM) show a strongly rectifying behavior for MoS_2 junction with n^- SiC, whereas the p^+ MoS_2/n^+ SiC junction exhibits an enhanced reverse current and a negative differential behavior under forward bias. This latter observation, indicating the occurrence of band-to-band-tunneling from the occupied states of n^+ SiC conduction band to the empty states of p^+ MoS_2 valence band, is a confirmation of the very sharp hetero-interface between the two materials. These results pave the way to the fabrication of ultra-fast switching Esaki diodes on 4H-SiC.

Introduction

In the last decade, silicon carbide (4H-SiC) emerged as the material of choice for power electronics, with a wide range of applications, such as sustainable mobility (automotive, trains, airplane) and renewable energy. Recently, SiC is also attracting and increasing interest for beyond power electronics applications, including digital electronics, optoelectronics and sensors [1]. In this context, the integration of two-dimensional (2D) materials with SiC can provide additional functionalities for these applications.

Molybdenum disulphide (2H-MoS_2) is a 2D layered semiconductor with interesting physical properties, such as a good electron mobility [2] and a layer-number dependent energy bandgap, with a transition from direct E_g=1.8-1.9 eV for a monolayer (1L) to indirect E_g=1.2 eV for few-layers (1L) MoS_2 [3]. In the last years, the integration of MoS_2 with SiC and GaN has been the object of increasing interest in optoelectronics (e.g., for the realization of high responsivity photodetectors covering the visible and UV spectral ranges) [4,5,6] and in electronics (e.g., for fast switching heterojunction diodes) [7,8,9,10]. The good lattice matching between the basal plane of MoS_2 with GaN and 6H- or 4H-SiC hexagonal crystals is favourable to the epitaxial growth of MoS_2 on these WBG materials. Hence, different deposition methods have been explored for the fabrication of 1L or few-layers MoS_2 heterostructures with GaN and SiC, including chemical vapour deposition (CVD) with vapours from S and MoO_3 powers [11], pulsed laser deposition (PLD) from a MoS_2 target [8], and the sulfurization of a pre-deposited ultra-thin MoO_x film [9,10]. In particular, the latter two-step growth approach is

highly compatible with semiconductor fab processes, and is suitable to achieve uniform MoS_2 coverage on large area (even on wafer scale), with a good control in the number of MoS_2 layers by setting the thickness of pre-deposited MoO_x film [12].
In this paper, we report a detailed structural, spectroscopic and electrical characterization of ultrathin MoS_2 films (predominantly formed by 1L) grown on the surface of two 4H-SiC(0001) 4°-off samples with different doping levels (i.e. a n^+ SiC substrate and a n- SiC epitaxy on n^+ substrate) by the sulfurization approach.

Experimental Details

A 4°-off n^+ doped 4H-SiC(0001) substrate ($N_D \approx 10^{19}$ cm^{-3}) and a n^- 4H-SiC epitaxy ($N_D \approx 10^{16}$ cm^{-3}) on the n^+ substrate were used in these experiments. MoO_x films were deposited on the 4H-SiC surface by DC sputtering from a Mo target and were converted to MoO_x by natural oxidation in air. The initial film thickness, evaluated by atomic force microscopy (AFM) step-height measurements, was ~1.2 nm. The sulfurization of the two samples was carried out in a two heating-zones furnace (as illustrated in Fig.1), with the zone 1 (at T=150°C) hosting S powders and zone 2 (at T=700 °C) hosting the sample, and the S vapours were transported by Ar carrier gas. The chemical properties of the sputter-deposited MoO_x films and the formation of MoS_2 after the sulfurization process were evaluated by X-ray photoelectron spectroscopy (XPS) using an XSAM 800 instrument by Kratos Analytical, with a Mg Kα X-ray source (1253.6 eV). High-angle annular dark field scanning transmission electron microscopy (HAADF-STEM) and energy dispersion spectroscopy (EDS) analyses of the MoS_2/4H-SiC heterojunctions were carried out with an aberration-corrected Titan Themis 200 microscope. Cross-sectioned samples were prepared by focused ion beam (FIB), after depositing a carbon/Pt protective layer on MoS_2 surface. Raman spectroscopy of MoS_2 vibrational peaks was carried out by a WiTec Alpha equipment, using a laser excitation at 532 nm and 100× objective. Morphological analyses by tapping mode AFM and nanoscale resolution current-voltage characterization of MoS_2/SiC heterojunctions by conductive AFM (C-AFM) were carried out with a DI3100 system by Bruker with Nanoscope V electronics. Pt-coated Si tips with a nominal curvature radius of ~5 nm were used for electrical measurements.

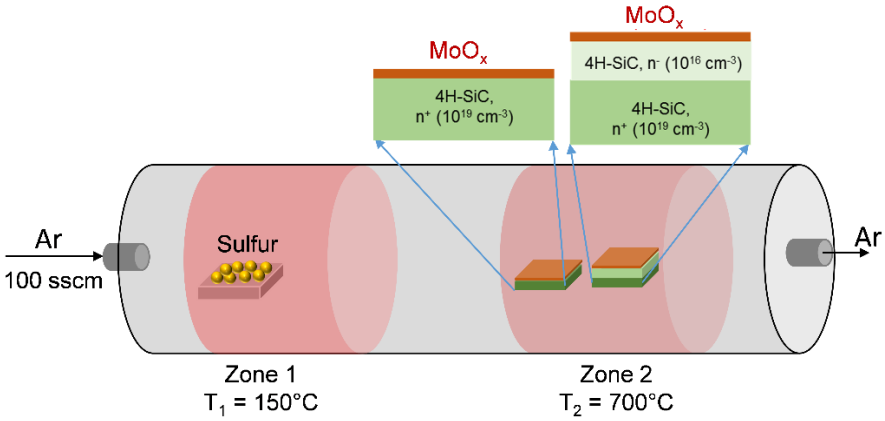

Fig. 1. Scheme of the two-heating zone furnace used for MoS_2 growth on n^+ 4H-SiC substrate and n- 4H-SiC epitaxy by sulfurization of pre-deposited ultra-thin MoO_x films.

Results and Discussion

The conversion of the thin MoO_x film into MoS_2 after the sulfurization process at 700 °C was preliminarily confirmed by XPS analyses. The positions of the Mo3d and S2s core level peaks in Fig.2 are consistent with the formation of MoS_2. However, deconvolution analysis of the spectra reveal the presence of MoO_3 residues in the film, which plays an important role as a source of p-type doping of MoS_2, as discussed later on in this paper.

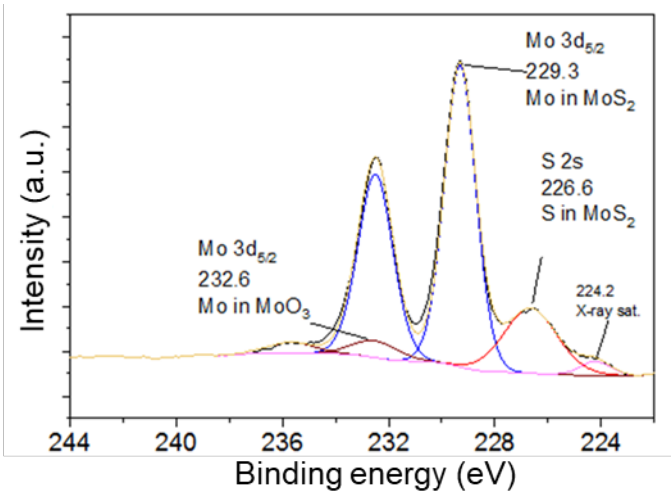

Fig.2. XPS core level Mo3d and S2s spectra, confirming the formation of MoS_2, with some MoO_3 residues, after the sulfurization process.

The structural and compositional properties of the MoS_2/4H-SiC heterojunctions were subsequently investigated with atomic scale resolution by cross-sectional HAADF-STEM and EDS mapping of the elemental species (Si, C, O, S and Mo), as illustrated in the Fig.3. These analyses confirms the formation of 1L-MoS_2 on 4H-SiC surface, without any reaction between Mo and SiC, and the formation of ~1 nm SiO_2 layer on SiC surface.

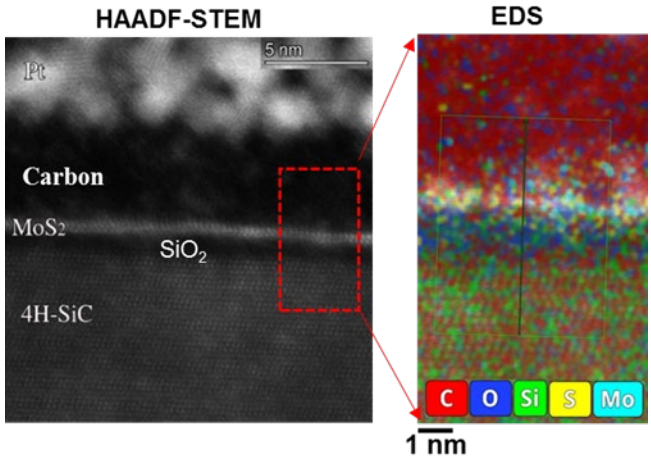

Fig.3. Cross-sectional HAADF-STEM (left) and EDS map of the Si, C, O, S and Mo elements (right) of as-grown 1L-MoS_2 on SiC.

Two representative micro-Raman spectra of MoS_2 grown on the n^+ SiC substrate and on the n^- SiC epitaxy are reported in Fig.4(a), where the characteristic vibrational modes E_{2g} and A_{1g} exhibit the same frequency and their separation $\Delta\omega$=20.1-20.3 cm^{-1} is compatible with 1L MoS_2 thickness. Fig.4(b) shows the histogram of the $\Delta\omega$ values extracted from a large array of Raman spectra collected at different positions of the laser spot on MoS_2 grown onto n^+ SiC surface. This statistical analysis confirms that the MoS_2 film coverage is uniform and it mainly consists of 1L, with a smaller 2L or 3L fraction. The variability of $\Delta\omega$ values in the 1L range (yellow box) is due to local variations of MoS_2 doping and strain. To further elucidate this aspect, Fig.4(c) shows a correlative plot of the A_{1g} and E_{2g} peaks frequencies [13] from the array of Raman spectra collected on the MoS_2/n^+ SiC. A small tensile strain (average value of ~0.12%) and a p^+-type doping (average holes density of 2.5×10^{12} cm^{-2}, corresponding to an average concentration $N_h\approx4\times10^{19}cm^{-3}$ for a MoS_2 thickness of ~0.65 nm) of 1L-MoS_2 was deduced from this analysis. The degenerate p^+-type doping of MoS_2 produced by the MoO_x sulfurization was ascribed to residues of MoO_3 in the film, as demonstrated by XPS

analyses in Fig.2. Very similar $\Delta\omega$ distributions and ω_{A1g} vs ω_{E2g} correlative plots were measured for MoS_2 grown on the n^- SiC epitaxy.

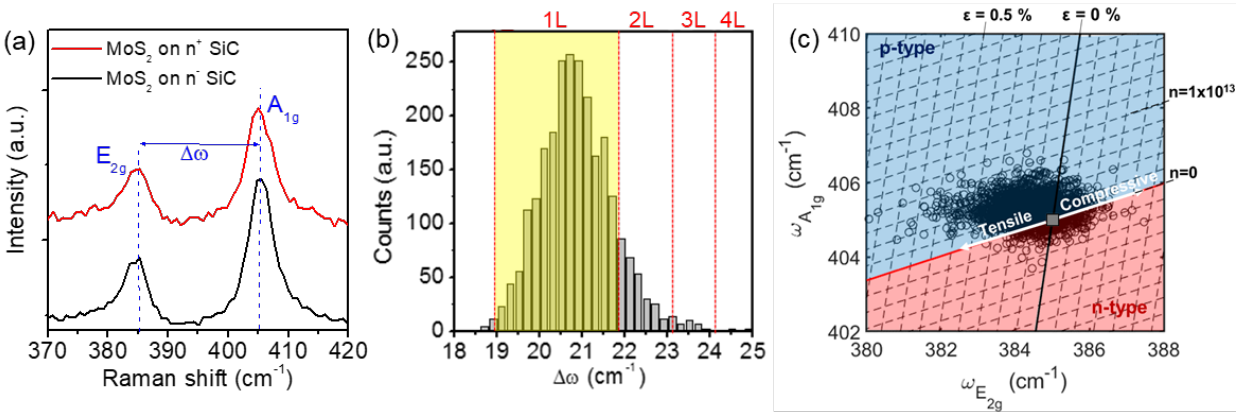

Fig.4. (a) Representative micro-Raman spectra of MoS_2 on n^+ SiC substrate and n- SiC epitaxy. (b) Correlative plot of the A_{1g} and E_{2g} peaks frequency for a large array of Raman spectra, from which p^+ doping and small tensile strain of 1L-MoS_2 is deduced.

Finally, the vertical current injection across the p^+ MoS_2 heterojunctions with n^- and n^+ doped 4H-SiC has been investigated by local current-voltage (I-V) characterization using the metal tip of conductive AFM, as illustrated in Fig.5(a) and (b), respectively.

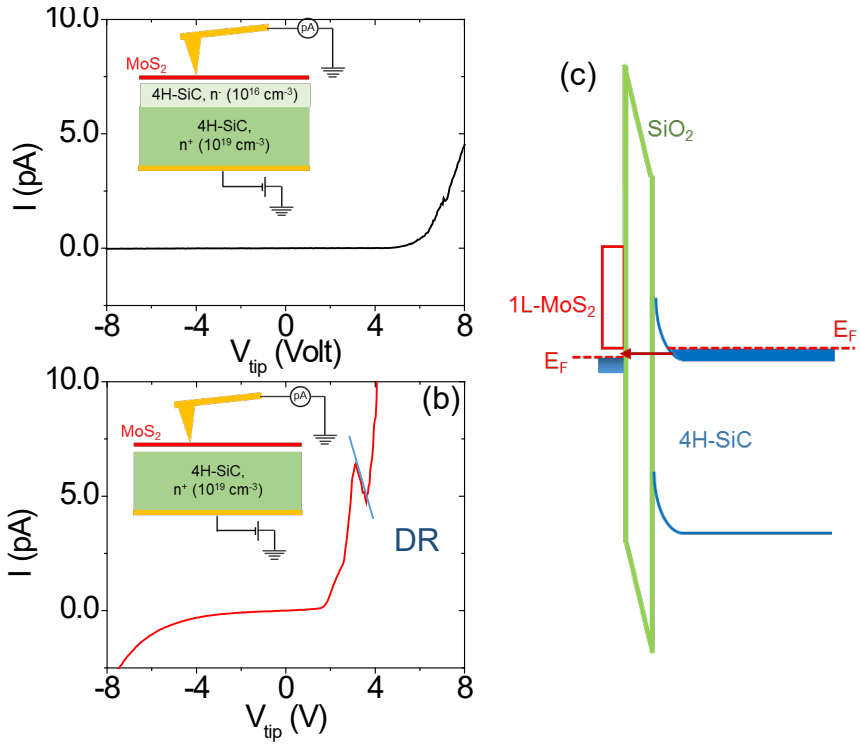

Fig.5. Representative I-V curves measured by C-AFM on 1L -MoS_2 heterojunctions with (a) the n^- 4H-SiC epitaxy and (b) the n^+ 4H-SiC substrate. The C-AFM setup is illustrated in the inserts. (c) Schematic band diagram of the p^+ MoS_2/n+ SiC heterojunction with the ultra-thin SiO_2 barrier layer in the BTBT configuration.

The p^+ MoS_2/ n^- SiC junction (Fig.5(a)) shows a rectifying behavior, with negligible current under negative bias and a current onset at high positive bias. On the other hand, I-V characteristics of the p^+ MoS_2/n^+ SiC (Fig.5(b)) exhibit an increased current under negative bias (due thermionic field emission or field emission through the thin depletion region of SiC) and the current onset at lower

positive bias values. Interestingly a negative differential resistance (NDR) is also observed under forward polarization. Such a phenomenon can be ascribed to the occurrence of band-to-band-tunneling (BTBT) at the interface between degenerately doped semiconductors, specifically from the filled stated of the n^+ SiC conduction band to the empty states of the p^+ MoS_2 valence band, as schematically illustrated in the band diagram of Fig.5(c). Such a behaviour, also called "Esaki diode" behavior, had been previously reported in homo-junction or heterojunction diodes of narrow bandgap semiconductors. To the best of our knowledge, this is the first observation of a NDR behaviour in 4H-SiC based diodes, and it is a demonstration of the very abrupt nature of the MoS_2 heterojunction with 4H-SiC. Further studies will be required to exploit this phenomenon in the fabrication of "Esaki diodes" for ultra-fast switching in 4H-SiC.

Summary

In conclusion, uniform MoS_2 films, mostly consisting of monolayers, have been grown on SiC surfaces with different doping levels (n^- SiC epitaxy with $N_D \approx 10^{16}$ cm^{-3} and n^+ SiC substrate with $N_D \approx 10^{19}$ cm^{-3}) by sulfurization of a pre-deposited ultra-thin MoO_x films. These films exhibit a very low tensile strain (~0.12%) and a p^+-type doping (average concentration $N_h \approx 4\times10^{19}$ cm^{-3}), ascribed to MoO_3 residues still present after the sulfurization process. The vertical current injection at the MoS_2/4H-SiC heterojunctions was investigated by nanoscale resolution I-V analyses with C-AFM. While a strongly rectifying behavior was observed for the junction with n^- SiC, the p^+ MoS_2/n^+ SiC junction exhibit an enhanced reverse current and a negative differential behavior under forward bias. This latter observation, indicating the occurrence of band-to-band-tunneling at the interface, is a confirmation of the very sharp heterointerface between the two materials. These results can open the way to the realization of ultra-fast switching Esaki diodes on 4H-SiC.

Acknowledgements

The authors acknowledge S. Di Franco (CNR-IMM) for the assistance in samples preparation, P. Fiorenza, G. Greco, M. Vivona and R. Lo Nigro (CNR-IMM) for useful discussions. The paper has been supported, in part, by MUR in the framework of the FlagERA- JTC 2019 project "ETMOS", by the CNR/HAS bilateral project GHOST-III (2023-25), and by European Union (NextGeneration EU), through the MUR-PNRR project SAMOTHRACE (ECS00000022).

References

[1] F. La Via, D. Alquier, F. Giannazzo, T. Kimoto, P. Neudeck, H. Ou, A. Roncaglia, S. E. Saddow, S. Tudisco, Micromachines 14 (2023) 1200.

[2] B. Radisavljevic, A. Radenovic, J. Brivio, V. Giacometti, A. Kis, Nat. Nanotechnol. 6 (2011) 147.

[3] Q. H. Wang, K. Kalantar-Zadeh, A. Kis, J. N. Coleman, M. S. Strano, Nat. Nanotechnol. 7 (2012) 699.

[4] C.-Y. Huang, C. Chang, G.-Z. Lu, W.-C. Huang, C.-S. Huang, M.-L. Chen, T.-N. Lin, J. L. Shen, T.-Y. Lin, Appl. Phys. Lett. 112 (2018) 233106.

[5] Y. Wu, Z. Li, K.-W. Ang, Y. Jia, Z. Shi, Z. Huang, W. Yu, X. Sun, X. Liu, D. Li, Photonics Res. 7 (2019) 1127.

[6] Y. Xiao, L. Min, X. Liu, W. Liu, U. Younis, T. Peng, X. Kang, X. Wu, S. Ding, D. W. Zhang, Nanophotonics 9 (2020) 3035.

[7] D. Ruzmetov, et al., ACS Nano 10 (2016) 3580.

[8] F. Giannazzo, S.E. Panasci, E. Schilirò, P. Fiorenza, G. Greco, F. Roccaforte, M. Cannas, S. Agnello, A. Koos, B. Pecz, M. Spankova, S. Chromik, Adv. Mater. Interf. 10 (2023) 2201502.

[9] F. Giannazzo, S.E. Panasci, E. Schilirò, F. Roccaforte, A. Koos, M. Nemeth, B. Pecz, Adv. Mat. Interf. 9 (2022) 2200915.

[10] F. Giannazzo, S.E. Panasci, E. Schilirò, G. Greco, F. Roccaforte, G. Sfuncia, G. Nicotra, M. Cannas, S. Agnello, E. Frayssinet, Y. Cordier, A. Michon, A. Koos, B. Pécz, Appl. Surf. Sci. 631 (2023) 157513.

[11] S. E. Panasci, I. Deretzis, E. Schilirò, A. La Magna, F. Roccaforte, A. Koos, B. Pécz, S. Agnello, M. Cannas, F. Giannazzo, Phys. Status Solidi RRL (2023) 2300218. DOI: 10.1002/pssr.202300218

[12] S. E. Panasci, A. Koos, E. Schilirò, S. Di Franco, G. Greco, P. Fiorenza, F. Roccaforte, S. Agnello, M. Cannas, F. M. Gelardi, A. Sulyok, M. Nemeth, B. Pécz, F. Giannazzo, Nanomaterials 12 (2022) 182.

[13] S. E. Panasci, E. Schilirò, G. Greco, M. Cannas, F. M. Gelardi, S. Agnello, F. Roccaforte, F. Giannazzo, ACS Appl. Mater. Interfaces 13 (2021) 31248.